Eur. Phys. J. B **15**, 657–663 (2000)

THE EUROPEAN PHYSICAL JOURNAL B

EDP Sciences

Single crystal study of the one dimensional $Ca_3Co_2O_6$ compound: five stable configurations for the Ising triangular lattice

A. Maignan[a], C. Michel, A.C. Masset, C. Martin, and B. Raveau

Laboratoire CRISMAT[b], ISMRA et Université de Caen, 6 boulevard du Maréchal Juin, 14050 Caen Cedex, France

Received 7 December 1999

Abstract. Single crystals of the one-dimensional phase $Ca_3Co_2O_6$ of several mm length have been grown. The magnetic study of such a crystal confirms the previous observations on polycrystalline samples: it consists of a triangular lattice of ferromagnetic $[Co_2O_6]$ chains ($T_{C1} = 24$ K) antiferromagnetically coupled ($T_{C2} = 12$ K). The dynamic of these chains array, probed by AC susceptibility, is very slow as shown from the large shift of the freezing temperature from 12 K to 16.5 K as the excitation frequency increases by three orders of magnitude (10^0 to 10^3 Hz). The origin of this effect is believed to be the result of different arrangements with close energies for the chain ferromagnetic moments on the triangular lattice. Five stable magnetic configurations have been evidenced by the magnetization as a function of applied field curves registered at 2 K. Their relative magnetizations correspond to $m = 1/4$, $1/2$, 1, 2, 3 where $m = 3$ represents the ferromagnetic ordering of three chains on the same triangle, each chain having a $m = 1$ magnetization. A magnetic phase diagram is finally proposed.

PACS. 75.50.y Studies of specific magnetic materials – 75.30.-m Intrinsic properties of magnetically ordered materials

1 Introduction

Cobalt oxides form a large family of compounds with fascinating structural and physical properties. The different possible oxidation states of cobalt - divalent, trivalent and tetravalent - together with its various spin configurations - for instance, low-spin, intermediate-spin and high- spin for Co^{3+} in a six-fold coordination [1] - are responsible for various original phenomena as temperature induced spin-state transitions in $LaCoO_3$ [1], giant magnetoresistance in $La_{1-x}Sr_xCoO_3$ [2] and insulator to metal transition and magnetoresistance properties in the oxygen deficient perovskites $LnBaCo_2O_{5.5}$ [3].

The lowering of the structural dimensionality of the cobalt oxides is susceptible to induce specific magnetic properties. This is illustrated by the Bi-based cobaltites $(Bi,Cd)_1Sr_2CoO_5$ [4] and $(Bi,Pb)_1Sr_3Co_2O_8$ [5] which exhibit a layered structure similar to the 1201 and 1212 type cuprates, and for which original magnetoresistance properties have been recently evidenced. Another spectacular effect of the bidimensionality upon magnetic properties was recently shown for $Ca_3Co_4O_9$, which exhibits a high figure of merit for the conversion of the thermoelectric energy [6].

The recent studies of the one-dimensional oxide $Ca_3Co_2O_6$ [7,8] are of great interest. They show that a transition from a ferrimagnetic (Fi) to a ferromagnetic (Fo) state is induced by a magnetic field. On the basis of this study performed on polycrystalline material, the authors could propose a rough magnetic phase diagram of $Ca_3Co_2O_6$. Nevertheless a single crystal study is absolutely necessary for further understanding of these magnetic properties. In this paper we report on the growth and magnetic properties of a single crystal of $Ca_3Co_2O_6$.

A previous structural study of polycrystalline $Ca_3Co_2O_6$ [9] has shown that the rhombohedral structure of this phase consists of $[Co_2O_6]_\infty$ chains running along the c axis of the corresponding hexagonal cell (Fig. 1a). In each chain, one CoO_6 octahedron alternates with one CoO_6 trigonal prism along c (Fig. 1b). The powder neutron diffraction study of this phase revealed a ferromagnetic intrachain exchange coupling ($J_{intra} > 0$) along c, whereas an antiferromagnetic (AF) interchain coupling ($J_{inter} > 0$) was observed on the (a, b) plane [7].

The long interchain Co-Co distance (5.3 Å), compared to the short Co-Co intrachain one (2.9 Å), explains the relationship between the magnetic exchange energies, $J_{intra} > J_{inter}$. Consequently, it is reasonable to describe the magnetism of $Ca_3Co_2O_6$ by considering a planar Ising triangular lattice where the magnetic moment of each chain plays the role of one spin. This scenario has been later confirmed by a magnetic study on ceramic samples, which has shown the existence of a magnetic field induced transition from Fi to Fo below T_{C1} [7,8]. Such a transition was predicted by the Ising triangular

[a] e-mail: antoine.maignan@ismra.fr
[b] UMR 6508

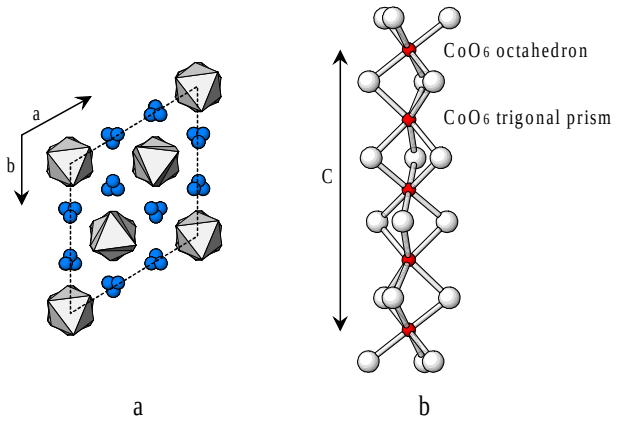

Fig. 1. (a) Projection onto (001) of the $Ca_3Co_2O_6$ structure showing the triangular arrangement of the chains, (b) $[Co_2O_6]_\infty$ chain evidencing the alternation of cobalt in octahedral and prismatic coordination.

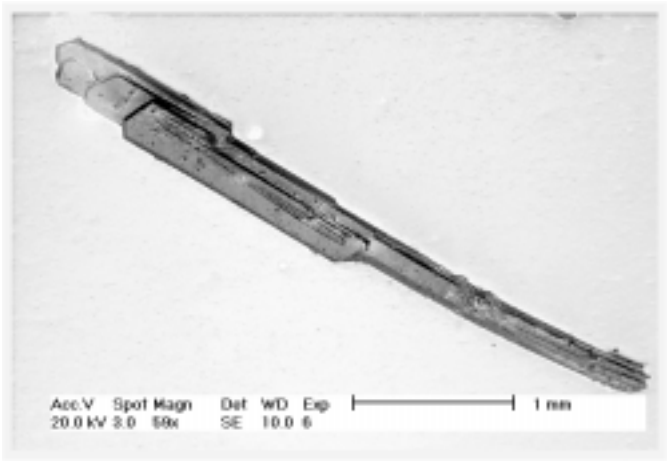

Fig. 2. $Ca_3Co_2O_6$ single crystal SEM micrograph.

network model [10]. Nevertheless, the magnetization maximum reached only 1.8 μ_B per Co mole [8], which could be explained by an intermediate spin configuration, $S = 1$, for trivalent cobalt. With the crystal growth of $Ca_3Co_2O_6$ we have been able to reinvestigate the physical properties of this 1D compound. In particular, AC-susceptibility and DC-magnetization measurements have been performed for an applied magnetic field parallel to the ferromagnetic chains. A very slow dynamic of the chain susceptibility is shown and several new substructures in the magnetization as a function of field curves are revealed at low temperatures ($T < 5$ K). A new magnetic phase diagram is proposed.

2 Experimental

2.1 Crystal growth

Single crystals were grown by heating a mixture of $Ca_3Co_4O_9$ and K_2CO_3, in a weight ratio 1/7, up to 880 °C for 48 h in an alumina boat in air and then cooling down to room temperature at 100 °C h^{-1}. In these conditions needle shaped crystals of several mm length are obtained (Fig. 2).

The X-ray diffraction study of the crystals confirms that their length coincides with the c axis of the hexagonal cell. Cationic analysis performed on numerous crystals by EDS technique shows the composition "Ca_3Co_2" without any contamination by potassium.

2.2 Transport and magnetic measurements

Resistivity measurements along the c axis of the single crystals, *i.e.* along the direction of the ferromagnetic chains, were carried out by four-probe method. Indium contacts were ultra sonically deposited.

AC susceptibility (AC-χ) and DC magnetic moment measurements were made with an AC-DC SQUID magnetometer. The AC-χ has been found to be independent of the AC magnetic field magnitude ($10^{-2}-10$ Oe), so that all the measurements were collected with $H_{ac} = 1$ Oe. The field and temperature dependent magnetization curves were collected with the DC field lying along the c axis of the crystals.

The magnetic anisotropy was checked by collecting the AC-χ data for the two geometries corresponding to $H \parallel c$ and $H \perp c$. However, a misalignment uncertainty of about 1° between the field direction and the crystal crystallographic axis cannot be excluded.

The high temperature susceptibility data were collected with a Faraday balance in 0.3 T by using powdered crystals.

3 Results and discussion

The high temperature properties, *i.e.* above the magnetic transition temperatures, have been probed by resistivity and susceptibility measurements. The resistivity (ρ) measured along the magnetic $[Co_2O_6]_\infty$ chains (c axis) of the $Ca_3Co_2O_6$ crystals as a function of temperature is given in Figure 3. The room temperature $\rho_{300\ K}$ value of $\approx 100\ \Omega$ cm and the negative value of the transport coefficient $d\rho/dT$ indicate the poor conducting behavior of the $[Co_2O_6]_\infty$ chains. This result is in agreement with the formal trivalent oxidation state of cobalt in this phase, implying a lack of carriers. The ρ data can be fitted with the variable range hopping (VRH) model, $\rho = A \exp(E/T^{1/1+n})$ [11], assuming the dimensionality n to be 1 (Fig. 3 upper x axis). The good quality of the VRH fitting confirms the localized character of the carriers in the $[Co_2O_6]_\infty$ chains. Note that the resistivity is too high to be measured perpendicularly to the chains.

In the temperature region where the crystal resistance can be measured, the application of a magnetic field up to 7 T does not modify the resistance. This absence of magnetoresistance is consistent with the $\chi^{-1}(T)$ data obtained

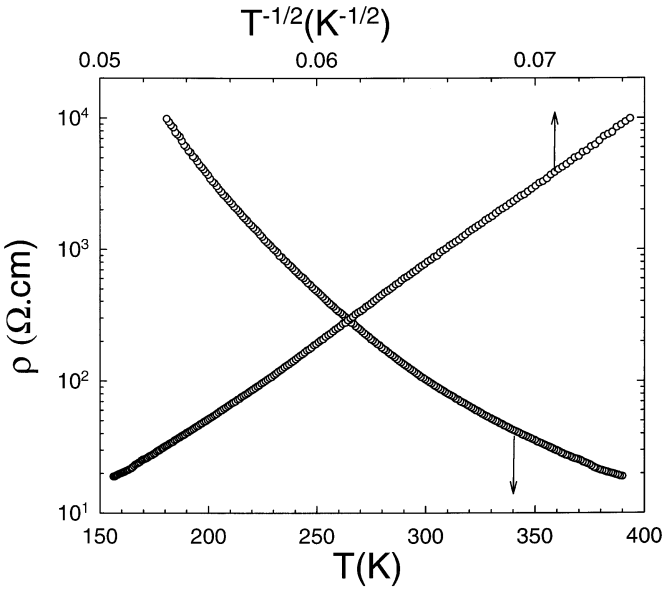

Fig. 3. T dependence of the resistivity ρ measured along the cobalt chains (lower x-axis). Corresponding $\rho(T^{-1/2})$ curve (upper x-axis).

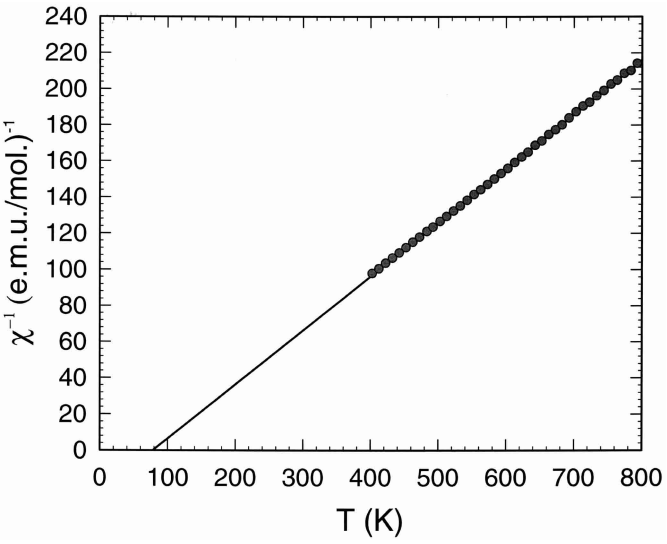

Fig. 4. T dependence of the inverse susceptibility (χ^{-1}) registered within 0.3 T. The straight line corresponds to the Curie-Weiss fitting.

from powdered crystals using a Faraday balance (Fig. 4). One indeed observes a linear T dependence for χ^{-1}, which can be fitted with the Curie Weiss law $\chi = C/(T+\theta_p)$ for $T > 400$ K, leading to $\theta_p \approx +80$ K and $\mu_{\text{eff}} \approx 3.8\ \mu_{\text{B}}$/mole Co, in perfect agreement with previous data [8]. Note however, that the μ_{eff} value is smaller than the theoretical value of 4.9 μ_{B} expected for a d^4 high spin configuration of trivalent cobalt. Such a difference can be explained by the ability of this cation to exhibit different spin states. The existence of two different crystallographic sites for cobalt -octahedral and trigonal prismatic- reinforces this hypothesis. A 1:1 mixture of high spin and intermediate spin configurations for trivalent cobalt at high temperature leads indeed to a calculated value $\mu_{\text{eff}} = 4\ \mu_{\text{B}}$, rather close to the experimental value.

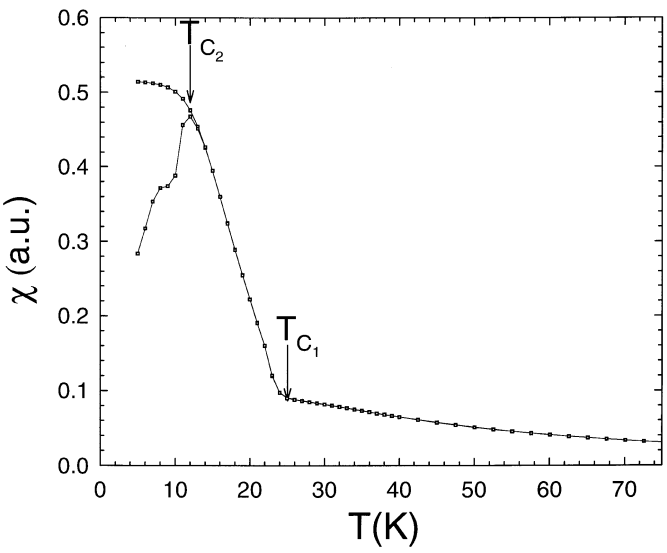

Fig. 5. zfc, fc $\chi(T)$ curve registered in 10^{-3} T with the field direction lying along the chains.

The $\chi(T)$ curve, registered at low temperature under 10^{-3} T upon cooling for a single crystal with the field parallel to the chains direction, reveals the existence of a magnetic transition at $T_{\text{C1}} = 24$ K, below which a sudden χ increase is observed (Fig. 5). This value for the crystal is in perfect agreement with the earlier value reported from a powder neutron diffraction study [7]. Moreover, a second magnetic transition occurs at $T_{\text{C2}} = 12$ K which corresponds to the merging temperature of the zero-field-cooling (zfc) and field-cooling (fc) $\chi(T)$ curves. The steep magnetization increase below T_{C1} corresponds to the intrachain Fo coupling of the Co cations, whereas the T_{C2} is the setting of the interchain AF coupling between the Fo chains and corresponds thus to the temperature of Fi ordering [7,8].

This first set of magnetic data for the $Ca_3Co_2O_6$ crystals confirms the previous results obtained with polycrystalline samples. This shows that, for this type of measurements, the random orientations of the crystallographic axis for the micro-crystals with respect to the field direction does not modify the main conclusions derived from these results. The origin of this similarity is the highly anisotropic nature of the magnetic properties of this 1D compound, which makes that all the macroscopic magnetic measurements reflect principally the $H \parallel c$ geometry. This is clearly demonstrated by the AC-$\chi(T)$ curves registered for two geometries corresponding to $H \parallel c$ and to $H \perp c$ (Fig. 6). Although these curves, registered with an excitation frequency of 1 Hz, exhibit a clear maximum at a temperature very close to T_{C2}, 11 K against 12 K (see Fig. 5), the χ' values for the $H \parallel c$ geometry are larger by a factor of 80, compared to $H \perp c$ configuration. This ratio is probably underestimated due to the possible alignment error for $H \perp c$. A 0.7° error is sufficient to explain this value if the magnetic anisotropy is infinite and this angle is in the uncertainty. This result obtained on a single crystal

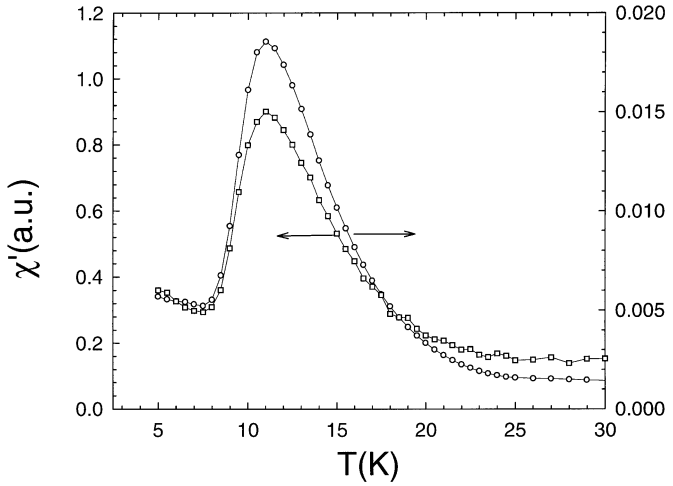

Fig. 6. $\chi'(T)$ curves for the geometries $H \parallel c$ (left y-axis) and $H \perp c$ (right y-axis).

shows that the magnetic moments of each chain are practically colinear with the latter, which validates the magnetism description by the Ising triangular model: a 2D triangular network of moments pointing perpendicularly to the triangles plane with an AF coupling between each moment and its nearest neighbors, from which the frustration originates. Compared to the conventional Ising triangular network [12], an additional difficulty for the magnetism arises from the unusual chain ferromagnetism since, as the field is reversed, one should flip an infinity of spins in each chain instead of only one spin in the case of the 2D Ising lattice. Thus the response time to field change should be much longer for the present compound than for the more simple Ising planar triangular lattice.

The AC-χ measurements are very useful to check the spins dynamic in the frustrated systems as for instance in the spin-glasses for which, by using different frequencies for $H_{\rm ac}$, the magnetic relaxation is probed [13]. Four frequencies, ranging from 1 to 10^3, covering three decades, have been used to study the response of the complex macroscopic susceptibility (χ', χ'') in the geometry $H \parallel c$ (Fig. 7). All the $\chi'(T)$ curves (Fig. 7a) show a shape very similar to the zfc magnetization $M(T)$ curve (Fig. 5), with a maximum value $\chi'_{\rm max}$ at $T_{\rm f}$, $\chi'_{\rm max}$ decreasing as the frequency increases. Moreover $T_{\rm f}$ is remarkably sensitive to the frequency, 11 K for 1 Hz (close to $T_{\rm C2} \approx 12$ K) to 16.5 K for 1 kHz. This huge $T_{\rm f}$ shift can also be measured from the $\chi''(T)$ curves (see inflexion points above the peak on Fig. 7b). It can be quantified by the coefficient $K = \Delta T_{\rm f}/\Delta(\log f)$, usually used to characterize the spin-glasses for which typical K values are in the range $5 \times 10^{-3} - 8 \times 10^{-2}$ [13]. The larger $K = 0.17$ value of the $Ca_3Co_2O_6$ crystal is closer to the value encountered for superparamagnetism ($K = 0.28$ in the a-$(Ho_2O_3)(B_2O_3)$ supermagnet). However, the steep magnetization rise below $T_{\rm C1}$, indicative of the intrachain ferromagnetic coupling, is not compatible with any paramagnetism. Large frequency effects on χ' (and χ'') have also been probed for cluster-glass materials such as $La_{0.5}Sr_{0.5}CoO_3$ but in

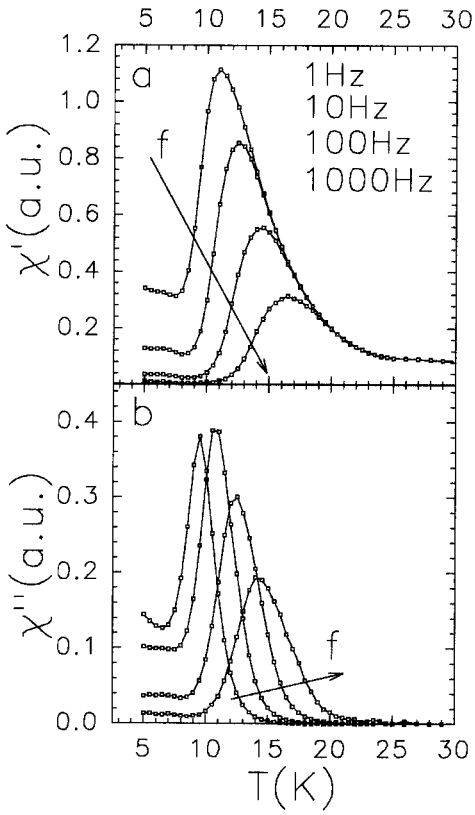

Fig. 7. (a) $\chi'(T)$ and (b) $\chi''(T)$ curves registered in the $H \parallel c$ geometry. The frequencies are labeled on the graph.

this case a large effect of the AC field amplitude was observed [14], in contrast to $Ca_3Co_2O_6$. The strong effect observed on the time range of the ms-s is more probably due to the frustration between the different magnetic configurations of the cobalt chains on the triangular lattice, which are frozen below $T_{\rm f}$. One consequence of the long chain magnetization reversal time is that the apparent susceptibility becomes nearly zero below $T_{\rm f}$ for the highest investigated frequency; this suggests that the magnetization is no longer able to follow the excitation field which yields 0 as an average value. The AF coupled 1D ferromagnetic chains on the Ising triangular lattice represent thus a rare opportunity to study the spin dynamics at a scale in between ms and s.

The magnetization measurements *versus* the applied magnetic field have only been performed for the $H \parallel c$ orientation. In order to avoid the magnetization dynamic effects revealed by the AC susceptibility, a quasi-equilibrated state has been reached by waiting 60 s after each field change prior to the measurement. Previous $M(H)$ measurements performed with different sweep rates have also demonstrated the crucial temporal effect on the results [8]. The $M(H)$ curves registered at low temperature from 12.5 K to 25 K (Fig. 8a) confirm the field induced Fi-Fo magnetic transition previously observed below the Fo temperature $T_{\rm C1} \approx 24$ K [7,8], and predicted

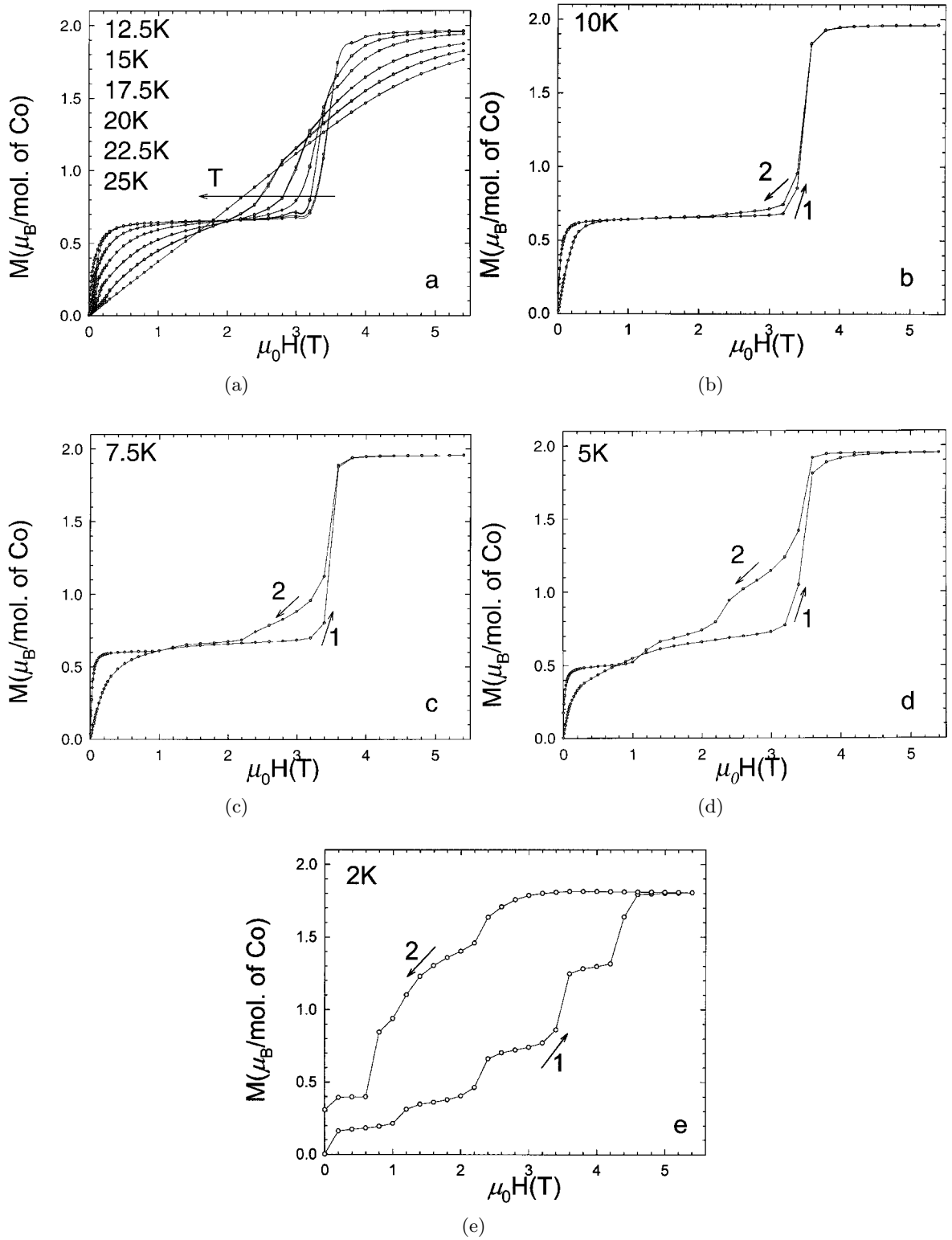

Fig. 8. $M(H)$ half loops. (a) $T = 12.5$ K to $T = 25$ K by 2.5 K step; (b) $T = 10$ K; (c) $T = 7.5$ K; (d) $T = 5$ K; (e) $T = 2$ K.

for the Ising triangular lattice [10]. The existence of a plateau in the Fi whose magnitude is 1/3 of the saturation magnetization in the Fo state is also shown. Nevertheless our isothermal $M(H)$ data on single crystal bring new features. Three temperature ranges can be discussed, taking into consideration the T_{C1} and T_{C2} temperatures. For $T \gg T_{C1}$, in agreement with the paramagnetic state of the compound, the curves are linear. Nevertheless, a small curvature can already be observed for $T = 25$ K, *i.e.* approximately 1 K above T_{C1} (Fig. 8a). For $T_{C2} < T < T_{C1}$, the intrachain ferromagnetic coupling is set up but the interchain AF coupling is still too weak to force the Fi installation. Consequently a partial AF state or a disordered state prevail in the absence of field. For this T interval, as the field increases, an induced magnetization plateau -more or less well defined- is always obtained whose magnitude corresponds to 1/3 of the saturation magnetization (Fig. 8a). Then beyond a critical field H_C, M jumps more or less abruptly to reach its saturation (Fi-Fo field induced transition). The magnetization maximum reaches 2 μ_B per mol of Co which can be explained by an intermediate spin for each Co^{3+} or a 1:1 mixture of high-spin and low-spin configurations. This latter hypothesis agrees with the magnetic neutron diffraction study [9] which shows 0.08 μ_B and 3 μ_B for cobalt in octahedral and prismatic coordination, respectively. In agreement with the lack of long range AF coupling for $T > T_{C2}$, the $M(H)$ half-loops are reversible. If one defines H_C as the inflexion point of the magnetic transition, one observes that H_C decreases as T increases beyond T_{C2}, from 3.6 T to 2.6 T for 12.5 K and 22.5 K, respectively (Fig. 8a). Simultaneously, the saturated magnetization decreases, as expected for a ferromagnet as T approaches the Curie temperature. At $T \approx T_{C2} \approx 12.5$ K, the Fi-Fo transition is very abrupt and reversible (Fig. 8a), whereas for $T < T_{C2}$ the transition remains abrupt but becomes irreversible as shown from the $M(H)$ curve at $T = 10$ K (Fig. 8b).

This shows that the free energies of the two Fi and Fo magnetic states are very close. The Fi - Fo reversibility for $T > T_{C2}$ is not indicative of a first order transition. Note that this field-induced transition in the crystal is much sharper than for the polycrystalline oxide. As T decreases below T_{C2} (Figs. 8b-8d), the $M(H)$ loops are characterized by two hysteretic parts, one around $H = 0$ which corresponds to the ferrimagnetic configuration, and the other near H_C which corresponds to the Fi-Fo transition. These irreversibilities are connected to the AF interchain coupling which is effective below T_{C2}, and thus which delays the spin reversal. For $T = 7.5$ K (Fig. 8c) and 5 K (Fig. 8d), the irreversibility is extended all over the magnetic field range except around 1 T.

Below 5 K the loops are totally irreversible, and moreover reveal new stable magnetic structures for this Ising triangular antiferromagnet. In particular for $T = 2$ K, two intermediate magnetization plateaus are observed before the 1/3 plateau is reached (Fig. 8e). If the magnetization of the Fo state is normalized to $M = 3$, *i.e.* each chain of a same triangle gets a $m = 1$ moment ($M = 3m$), these two new substructures of the $M(H)$ loop well defined at 2 K correspond to $M = 1/4$ and $M = 1/2$. Remarkably, a fourth plateau is also observed for $H > H_C$ whose magnetization value corresponds to $M = 2$. By varying the magnetic field between 0 and 5.5 T, five different magnetic configurations can thus be stabilized at $T = 2$ K. Depending upon the magnetic field, the normalized magnetization values can be $M = 0$, 1/4, 1/2, 1, 2, 3. This illustrates the variety of magnetic structures that can be encountered in this frustrated magnetic triangular network. All these underlying different configurations in zero field are probably at the origin of the large frequency dependence revealed in the AC-susceptibility measurements, the competition between these different magnetic states of close energies being at the origin of a large degree of frustration.

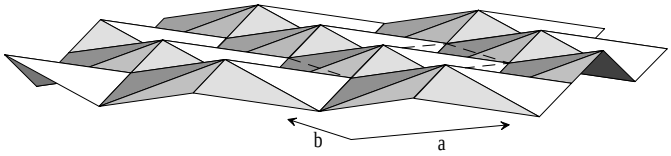

Fig. 9. Buckling array of "Co_3" triangles parallel to the (a, b) plane. In each triangle, apices are nearest cobalt atoms between neighbouring Co_2O_6 chains.

To the best of our knowledge, these new and stable magnetic states have not been predicted and are observed for the first time. They can be explained by using a description, which involves interactions at longer scales than the first nearest neighbors. Some peculiarities of the $Ca_3Co_2O_6$ structure, among which the existence of two different cobalt sites alternating in the same $[Co_2O_6]_\infty$ chain, may be at the origin of the stabilization of these substructures. In fact the "Co_3" triangles are not exactly perpendicular to the chains and thus form a buckling array of triangles (Fig. 9) roughly parallel to the (a, b) plane. Each "Co_3" triangle contains indeed only two equivalent crystallographic sites out of three, *i.e.* two octahedral and one prismatic cobalt or *vice versa*.

Finally, such a single crystal study allows a more detailed magnetic phase diagram (Fig. 10) to be proposed. Four domains can be distinguished, corresponding to the paramagnetic (PM), disordered antiferromagnetic (DIS), ferrimagnetic (Fi) and ferromagnetic (Fo) states. An important characteristic of this diagram concerns the dashed area below 5 K, which shows irreversibility properties, and where new magnetic substructures are evidenced. In order to explain these different magnetic substructures with $M = 0$, 1/4, 1/2, 1, 2, and 3, different magnetic models involving "Co_3" triangles can be proposed (Fig. 11). These models suppose that in each linear chain (each apex of triangles), the ferromagnetic ordering is perfectly established leading to a normalized magnetic moment ± 1. Consequently for each triangle the magnetic moment is equal to -1, +1 or +3 (inset of Fig. 11).

In their study based on neutron powder diffraction, Aasland *et al.* [7] have shown that the $M = 1$ structure (Fi) can be described by the arrangement given in

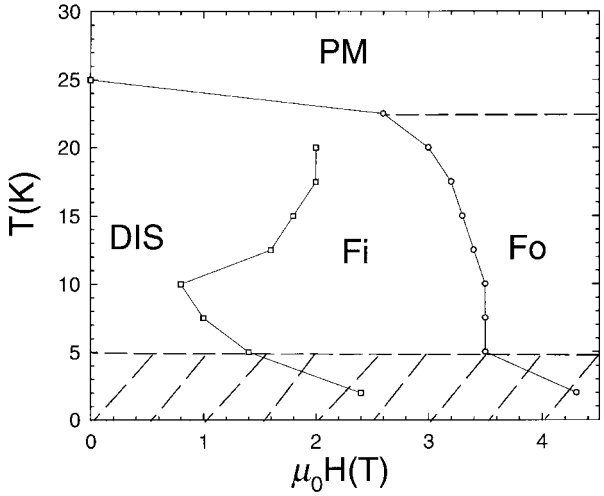

Fig. 10. Magnetic phase diagram PM, DIS, Fi and Fo are for paramagnetic, disordered magnetic state, ferrimagnetic and ferromagnetic. The dashed area corresponds to the irreversible region consisting of different magnetic substructures.

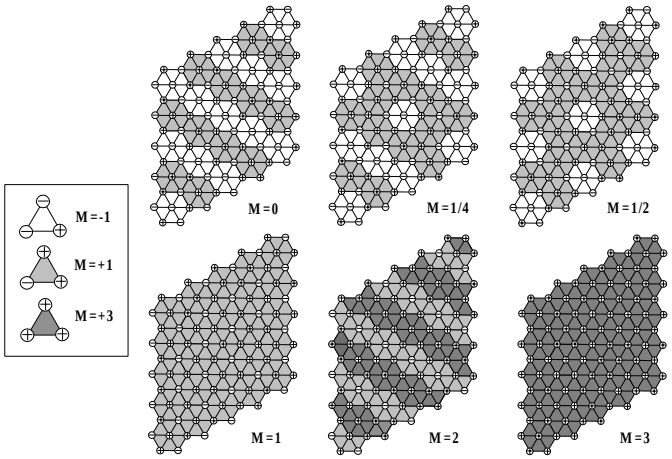

Fig. 11. Possible models explaining the different observed magnetic structures. The magnetic moment of individual triangles depends on the orientation of the magnetic moment of the ferromagnetic chains (apices), the three possible values are schematized by different colors (defined in inset).

Figure 11. Two kinds of chains are observed, in the hexagonal unit cell: among the three chains, one has a spin down (-) and is surrounded by six spins up (+) and the other two have spin (+) with half neighbors spin up and down. Another way to describe this arrangement is to consider the 2D hexagonal array by using "Co_3" triangles. The magnetic moment of each triangle is $M = +1$ in this case ($M = 1$ in Fig. 11). We have tried to describe the intermediate substructure between this $M = +1$ (Fi) state and the $M = +3$ (Fo) limit model (Fig. 11). As the magnetic field is applied in the + direction, the magnetic moment of several chains flips progressively. Since each Co chain is common to six "Co_3" triangles, it turns out that as the moment of one chain flips up, the M value of the six adjacent triangles forming an hexagon increases from +1 to +3. Applying this model in a regular way on half of the (-) spin of the M =+1 configuration we obtain the $M = +2$ configuration proposed in Figure 11. Based on this mechanism, one can start from M =+3 and finish to $M = 0$, as proposed in Figure 11, with intermediate substructures corresponding to the steps observed on the magnetization curves at low temperature. A neutron diffraction study, as a function of magnetic field and below 5 K, is necessary in order to check the existence of such superstructures with long range ordered magnetic moment on the "Co_3" triangles.

References

1. M.A. Senaris-Rodriguez, J.B. Goodenough, J. Solid State Chem. **116**, 224 (1995); *ibid.* **118**, 323 (1995).
2. G. Briceno, H. Chang, X. Sun, P.G. Schultz, X.D. Xiang, Science **270**, 273 (1995).
3. C. Martin, A. Maignan, D. Pelloquin, N. Nguyen, B. Raveau, Appl. Phys. Lett. **71**, 1421 (1997).
4. D. Groult, C. Martin, A. Maignan, D. Pelloquin, B. Raveau, Solid State Commun. **105**, 583 (1998).
5. T. Yamamoto, I. Isukada, K. Uchinokura J. Appl. Phys. **38**, 1949 (1999).
6. L. Li, R. Funakaski, I. Matsubara, K. Ueno, H. Yamada, J. Mater. Chem. **9**, 1959 (1999).
7. S. Aasland, H. Fjellvag, B. Hauback, Solid State Commun. **101**, 187 (1997).
8. H. Kageyama, K Yoshimura, K. Kosuge, H Mitamura, T. Goto, J. Phys. Soc. Jpn **66**, 1607 (1997).
9. H. Fjellvag, E. Gulbrandsen, S. Aasland, A. Olsen, B. Haubach, J. Solid State Chem. **124**, 190 (1996).
10. S. Migashita, J. Phys. Soc. Jpn **55**, 3605 (1986).
11. N.F. Mott, Metal insulator transitions, 2nd edn. (Taylor & Francis, London, 1974).
12. M. Mekata, J. Phys. Soc. Jpn **42**, 76 (1977).
13. J.A. Mydosh, *Spin Glasses* (Taylor & Francis, London, 1993).
14. S. Mukherjee, R. Ranganathan, P.S. Anilkumar, P.A. Joy, Phys. Rev. B **54**, 9267 (1996).